



# PERFORMANCE ANALYSIS OF TERAHERTZ WIRELESS COMMUNICATION



## PROJECT REPORT

*Submitted by*

**VANMATHI J**

**Register No: 15MCO013**

*in partial fulfillment for the requirement of award of the degree*

*of*

**MASTER OF ENGINEERING**

*in*

**COMMUNICATION SYSTEMS**

**Department of Electronics and Communication Engineering**

**KUMARAGURU COLLEGE OF TECHNOLOGY**

(An autonomous institution affiliated to Anna University, Chennai)

**COIMBATORE-641049**

**ANNA UNIVERSITY: CHENNAI 600 025**

**APRIL 2017**

## **BONAFIDE CERTIFICATE**

Certified that this project report titled “**PERFORMANCE ANALYSIS OF TERAHERTZ WIRELESS COMMUNICATION**” is the bonafide work of **VANMATHI J [Reg. No. 15MCO013]** who carried out the research under my supervision. Certified further, that to the best of my knowledge the work reported herein does not form part of any other project or dissertation on the basis of which a degree or award was conferred on an earlier occasion on this or any other candidate.

### **SIGNATURE**

**Dr.M.BHARATHI**

### **PROJECT SUPERVISOR**

Department of ECE

Kumaraguru College of Technology

Coimbatore-641 049

### **SIGNATURE**

**Prof. K. RAMPRAKASH**

### **HEAD OF PG PROGRAMME**

Department of ECE

Kumaraguru College of Technology

Coimbatore-641 049

The Candidate with **Register No. 15MCO013** was examined by us in the project viva –voce examination held on.....

**INTERNAL EXAMINER**

**EXTERNAL EXAMINER**

## ACKNOWLEDGEMENT

First, I would like to express my praise and gratitude to the Lord, who has showered his grace and blessings enabling me to complete this project in an excellent manner.

I express my sincere thanks to the management of Kumaraguru College of Technology and Joint Correspondent **Shri Shankar Vanavarayar** for the kind support and for providing necessary facilities to carry out the work.

I would like to express my sincere thanks to our beloved Principal **Dr.R.S.Kumar**, Kumaraguru College of Technology, who encouraged me with his valuable thoughts.

I would like to thank **Prof. K. Ramprakash**, Head of PG programme, Electronics and Communication Engineering, for his kind support and for providing necessary facilities to carry out the project work.

I am greatly privileged to express my heartfelt thanks to my project guide and project coordinator **Dr.M.Bharathi**, Professor, Department of Electronics and Communication Engineering, for her expert counseling and guidance to make this project to a great deal of success.

I wish to convey my deep sense of gratitude to all teaching and non-teaching staff of ECE Department for their help and cooperation.

Finally, I thank my parents and my family members for giving me the moral support and abundant blessings in all of my activities and my dear friends who helped me to endure my difficult times with their unfailing support and warm wishes.

# ABSTRACT

Terahertz Band (0.1-10 THz) communication is envisioned as a key technology to satisfy the increasing demand for ultra-broadband wireless communication. Terahertz communication is 1000 times faster than the current wireless communication. The achievable data rate is in the order of Tbps. Now currently THz band is used for space applications, THz band is used in the inter-satellite link for high capacity transmission.

The physical mechanisms governing a wireless transmission in the 0.1 – 10 THz band are a very high molecular absorption and spreading loss which result in a very high and frequency-selective path loss for the Line-Of-Sight (LOS) links. For the Non-Line-Of-Sight (NLOS) propagation, high reflection loss depending on the shape, material, and roughness of the reflecting surface affects the THz wave propagation.

In this project, LOS propagation model is developed by adopting a molecular High Resolution Transmission (HITRAN) database which accounts the values for the fraction of water vapor in the air. NLOS propagation model is developed based on the Kirchhoff scattering theory and ray tracing algorithm. By considering these two propagation path, the equivalent channel model for the indoor scenario is developed. Due to the constructive and destructive superposition of the numerous reflected paths and the direct path, fluctuations of the Channel Transfer Functions (CTF) are observed. For the indoor scenarios the LOS component dominates over the entire band from 0.1 THz to 10 THz with a path gain of -41 dB to -70 dB.

Frequency Domain-Differential Phase Shift Keying (FD-DQPSK) modulation is developed over this band, and the Symbol Error Rate (SER) is obtained. For small distances (<2m), the SER is sufficiently low, but for increase in distance, the achieved SER is not sufficient. The adaptive FD-DQPSK modulation scheme is implemented to reduce symbol error rate and it achieves better result than the FD-DQPSK.

# TABLE OF CONTENTS

<b>CHAPTER NO</b>	<b>TITLE</b>	<b>PAGE NO</b>
	<b>ABSTRACT</b>	<b>iv</b>
	<b>LIST OF FIGURES</b>	<b>Vii</b>
	<b>LIST OF TABLES</b>	<b>ix</b>
	<b>LIST OF ABBREVIATIONS</b>	<b>x</b>
<b>1</b>	<b>INTRODUCTION</b>	<b>1</b>
	1.1 Terahertz radiations	1
	1.1.1 sources of terahertz radiation	2
	1.1.2 Terahertz application	3
	1.2 Channel Characteristics	4
	1.2.1 Channel Loss	4
<b>2</b>	<b>LITERATURE REVIEW</b>	<b>6</b>
	2.1. Review On Terahertz Communication	6
	2.2. Review On Channel Model	8
<b>3</b>	<b>CHANNEL MODELING</b>	<b>10</b>
	3.1 Channel Model	10
	3.1.1 Line Of Sight Propagation	10
	3.1.1.1 HITRAN	11
	3.1.2 Non Line Of Sight Propagation	12
	3.1.2.1 Kirchhoff Scattering Theory	13
	3.1.2.2 Ray Tracing Algorithm	15
	3.1.3 Equivalent Channel Model	16
	3.2 Capacity Analysis	17

<b>4</b>	<b>MODULATION SCHEMES</b>	<b>19</b>
	4.1 Modulation	19
	4.1.1 pulse modulation scheme	20
	4.1.1.1 FD-DQPSK	20
	4.1.1.2 Adaptive FD-DQPSK	26
<b>5</b>	<b>SIMULATION RESULTS</b>	<b>27</b>
<b>6</b>	<b>CONCLUSION AND FUTURE WORK</b>	<b>36</b>
	<b>REFERENCES</b>	<b>37</b>
	<b>LIST OF PUBLICATIONS</b>	<b>39</b>

## LIST OF FIGURES

FIGURE NO	TITLE	PAGE NO
1.1	Terahertz radiations in the Electromagnetic spectrum	2
3.1	The basic geometry of scattering at a rough surface.	13
3.2	Division of the scattering surface in square tiles	15
4.1	Transmitter block diagram	22
4.2	Receiver block diagram	23
5.1	Absorption coefficient Vs Wave number for 278 Kelvin	28
5.2	Absorption coefficient Vs Wave number for 308 Kelvin	29
5.3	Total path losses Vs Frequency for 278 Kelvin	30
5.4	Total path losses Vs Frequency for 308 Kelvin	31
5.5	Reflection power Vs Frequency	32
5.6	Channel Transfer Function Vs Frequency	33

5.7	Average Channel Capacity for LOS, NLOS, Equivalent path	34
5.8	SER for FD-DQPSK and Adaptive FD-DQPSK	35



## **LIST OF TABLES**

<b>TABLE NO</b>	<b>TITLE</b>	<b>PAGE NO</b>
5.1	Simulation parameter	27

## LIST OF ABBREVIATIONS

LOS	Line Of Sight
NLOS	Non Line Of Sight
HITRAN	High Resolution Transmission
EM	Electro Magnetic
TX	Transmitter
RX	Receiver
CTF	Channel Transfer Function
ASK	Amplitude Shift Keying
PSK	Phase Shift Keying
FSK	Frequency Shift Keying
PSD	Power Spectral Density
BER	Bit Error Rate
SER	Symbol error rate
SNR	Signal to noise ratio
FD-DPSK	Frequency Domain Differential Phase Shift Keying

# CHAPTER 1

## INTRODUCTION

Wireless data traffic has exponentially grown in the past years, and this has been accompanied by an increasing demand for higher speed wireless communication. In particular, wireless data rates have doubled every eighteen months over the last three decades. Terahertz (0.1–10 THz) band communication is envisioned as a key technology to satisfy this increasing demand for ultra-broadband wireless communication. THz Band communication will alleviate the spectrum scarcity and capacity limitations of current wireless system. Terahertz communication is 1000 times faster than the current wireless communication, it can achieve data rate of 1 Tbps. In this chapter, a brief overview of THz radiation is discussed, along with the channel characteristics at THz band.

### 1.1 TERAHERTZ RADIATION

Terahertz radiation also known as sub millimeter radiation, it consists of electromagnetic waves within the ITU-designated band of frequencies from 0.1 to 10 terahertz[1]. Wavelengths of radiation in the terahertz band correspondingly range from  $1\mu\text{m}$  to  $100\mu\text{m}$ . Because terahertz radiation begins at a wavelength of one millimeter and proceeds into shorter wavelengths, it is sometimes known as the sub millimeter band and its radiation as sub millimeter waves. Terahertz radiation falls in-between infrared radiation and microwave radiation in the electromagnetic spectrum as shown in the Figure 1.1, and it shares some properties with each of these. Like infrared and microwave radiation, terahertz radiation travels in a line of sight and is non-ionizing. Like microwave radiation, terahertz radiation can penetrate a wide variety of non-conducting materials. Terahertz radiation can pass through clothing, paper, cardboard, wood, masonry, plastic and ceramics. The penetration depth is typically less than that of microwave radiation. Terahertz radiation has limited penetration through fog and clouds and cannot penetrate liquid water or metal. The earth's atmosphere is a strong absorber of terahertz radiation in specific water vapor absorption bands, so the range of terahertz radiation is limited enough to

affect its usefulness in long-distance communications. However, at distances of 10 meters the band may still allow many useful applications in imaging and construction of high bandwidth wireless networking systems, especially indoor systems. In addition, producing and detecting coherent terahertz radiation remains technically challenging, though inexpensive commercial sources now exist in the 0.1–10 THz range (the lower part of the spectrum), including gyrotrons, backward wave oscillators, and resonant-tunneling diodes.

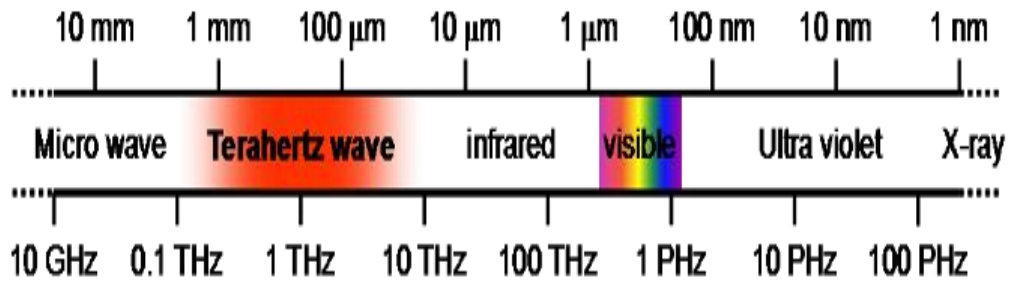


Figure 1.1 Terahertz radiations in the electromagnetic spectrum

### 1.1.1 SOURCES OF TERAHERTZ RADIATION

#### Natural sources

Terahertz radiation is emitted as part of the black-body radiation from anything with temperatures greater than about 10 Kelvin. While this thermal emission is very weak, observations at these frequencies are important for characterizing the cold 10–20K dust in the interstellar medium in the Milky Way galaxy, and in distant starburst galaxies.

#### Artificial sources

Single-cycle or pulsed sources used in terahertz time domain spectroscopy such as photoconductive, surface field and optical rectification emitters. Electronic oscillators based on resonant tunneling diodes have been shown to operate up to 700 GHz.

Argonne National Laboratory created a compact device that could lead to portable, battery-operated terahertz radiation sources. The device uses high-temperature superconducting

crystals, which comprise stacks of Josephson junctions, which exhibit a property known as the Josephson effect. When external voltage is applied, alternating current flows across the junctions at a frequency proportional to the voltage. This alternating current induces an electromagnetic field. Even a small voltage can induce frequencies in the terahertz range.

The engineers at Harvard University achieved room temperature emission of several hundred nanowatts of coherent terahertz radiation using a semiconductor source. THz radiation was generated by nonlinear mixing of two modes in a mid-infrared quantum cascade laser.

The researchers at Georgia Institute of Technology's Broadband Wireless Networking Laboratory and the Polytechnic University of Catalonia developed a method to create a graphene antenna: an antenna that would be shaped into graphene strips from 10 to 100 nanometers wide and one micrometer long. Such an antenna would broadcast in the terahertz frequency range.

### **1.1.2 TERAHERTZ APPLICATION**

Terahertz radiations are used in many research fields they are medical imaging, safety, scientific use and imaging, communication, manufacturing, and power generation.

#### **Medical Imaging**

Terahertz radiation is not ionizing radiation and its low photon energies in general do not damage tissues and DNA. Some frequencies of terahertz radiation can penetrate several millimeters of tissue with low water content (e.g., fatty tissue) and reflect back. Terahertz radiation can also detect differences in water content and density of a tissue. Such methods could allow effective detection of epithelial cancer with an imaging system that is safe, non-invasive, and painless. Some frequencies of terahertz radiation can be used for 3D imaging of teeth and may be more accurate than conventional X-ray imaging in dentistry.

#### **Security**

Terahertz radiation can penetrate fabrics and plastics, so it can be used in surveillance, such as security screening, to uncover concealed weapons on a person, remotely. This is of particular interest because many materials of interest have unique spectral "fingerprints" in the terahertz range. This offers the possibility to combine spectral identification with imaging.

The compact sized THz camera for security screening applications, imaged guns and explosives concealed under clothing. Passive detection of terahertz signatures avoid the bodily privacy concerns of other detection by being targeted to a very specific range of materials and objects.

### **Scientific use and Imaging**

THz time-domain spectroscopy (THz TDS) and THz tomography are able to perform measurements on, and obtain images of, samples that are opaque in the visible and near-infrared regions of the spectrum. THz-TDS produces radiation that is both coherent and spectrally broad, so such images can contain far more information than a conventional image formed with a single-frequency source.

### **Manufacturing**

Many possible uses of terahertz sensing and imaging are proposed in manufacturing, quality control, and process monitoring. These in general exploit the traits of plastics and cardboard being transparent to terahertz radiation, making it possible to inspect packaged goods.

### **Power Generation**

NASA has done recent work with using terahertz radiation in the "5-30THz range" to vibrate a nickel lattice loaded with hydrogen in order to induce low energy nuclear reactions but has found that generating the radiation using existing technologies to be very inefficient

## **1.2 CHANNEL CHARACTERISTICS**

The characteristic of free space at THz band includes various losses and are discussed.

### **1.2.1 CHANNEL LOSSES**

The channel losses in the terahertz band are spreading loss, absorption loss and reflection loss.

Spreading loss is the loss in signal strength of an electromagnetic wave that would result from a line-of-sight path through free space (usually air), with no obstacles nearby to cause reflection or diffraction. It does not include factors such as the gain of the antennas used at the transmitter and receiver, nor any loss associated with hardware imperfections. Spreading loss is proportional to the square of the distance between the transmitter and receiver, and also proportional to the square of the frequency of the radio signal. A transmitted signal attenuates over distance because the signal is being spread over a larger and larger area. This form of attenuation is known as free space loss.

The absorption loss is depends on the signal frequency and the atmospheric gases. In the THz band, the absorption level of atmospheric gases is very strong which is caused by molecular resonances primarily due to water vapor and oxygen [9]. The molecular absorption is caused by the transmitted EM wave is shifting the molecules in the medium to higher energy states. The energy, equivalent to the difference between the higher and the lower energy state of a molecule, determines the absorption energy that is drawn from the EM wave. This has a direct impact on the absorption frequency as the absorbed energy is  $E = hf$ , where  $h$  is the Planck's constant and  $f$  is frequency. The absorption coefficient depends on frequency and gives the THz band a very peculiar frequency selective spectral absorption profile.

In an indoor scenario, the propagation path might be reflected by the presence of obstacles like moving people, furniture, or many diverse objects [12]. The signal power is scattered at the time of reflection. This attenuation is called reflection loss. The characteristics of the reflection are governed by the scattering coefficient  $\rho$ . Scattering loss is depends on the roughness factor of the reflected material.

The transmission distance of ultrahigh-speed THz communication is very limited due to the very high path loss in the terahertz channel. But it offers high bandwidth with several gigahertz wide transmission windows, so it achieves high data rate. The objective of this project is to model the THz channel and to analyze the symbol error rate performance using adaptive frequency domain differential phase shift keying modulation (FD-DQPSK).

## **CHAPTER 2**

### **LITERATURE REVIEW**

Terahertz frequency for communication is explained by researcher in the recent past. THz channel is quite different from the current wireless channel. So simulation of the channel is a important first step towards the use of THz band for communication. A brief review of the existing channel modeling in the THz range is presented in this chapter.

#### **2.1 REVIEW ON TERAHERTZ COMMUNICATION**

Akyildiz and Jornet [1], discussed the Terahertz Band (0.1–10 THz) communication and the in-depth view of device design and development challenges for THz Band [1]. The limitations and possible solutions for high-speed transceiver architectures are highlighted. The challenges for the development of new ultra-broadband antennas and very large antenna arrays are explained. When the devices are finally developed, then they need to communicate in the THz band. There exist many novel communication challenges such as propagation modeling, capacity analysis, modulation schemes, and other physical and link layer solutions. Some applications of the terahertz band at the macro scale and the micro scale are explained.

Song and Nagatsuma [2], highlighted the present and future terahertz communication. In present technologies for THz communications it focus on channel modeling, device technologies for the front-end, and demonstrations for testing the feasibility of THz communications. THz communications offers an alternative for future wireless communications systems, especially for indoor applications such as WLANs and WPANs. Although high-gain antennas should probably be employed because of the large free-space loss at THz frequencies, the huge bandwidth of THz waves will enable to achieve data rates of 10 Gbps or higher easily even with simple data modulation.



Farnoosh Moshir and Suresh Singh, explained the problem of building a communication channel based on modulation of terahertz pulses [3]. The channel model based on measurements carried out on a terahertz time-domain system is developed. Frequency domain differential quadrature phase shift keying (FD-DQPSK) and Adaptive FD-DQPSK pulse modulation schemes are implemented. These modulation schemes results the data rates of about 1 Tbps for distances of up to three meters.

Anamaria Moldovan and Steven Kisseleff [4], they considered the design of uncoded point-to-point THz transmission systems using realistic transmit, receive, and equalization filter. The problem of equalizing a very long dispersive channel impulse response by utilizing a frequency-division based scheme with multiple sub-bands is highlighted. The iterative power allocation algorithm is developed to maximize the data rate.

Cheng Wang and Changxing Lin, describes a 140-GHz wireless link whose maximum transmission data rate is 10 Gbit/s[5]. A high-performance transmitting and receiving front end is developed by sub-harmonic mixer and multiplier based on Schottky barrier diodes, a waveguide H ladder bandpass filter, a Cassegrain antenna. 16 quadrature amplitude modulation is adopted to improve the spectrum efficiency. 32-way parallel demodulation architecture based on frequency-domain implementation of the matched filter and timing phase correction is modeled. An adaptive blind equalization algorithm is also realized to enhance the tolerance for channel distortion.

Lothar Moeller and John Federici ,developed a novel scheme for generating a 2.5 Gb/s data signal on a 625 GHz carrier, its transmission over lab distance, and error-free detection[6]. Duobinary baseband modulation on the transmitter side generates a signal with a sufficiently narrow spectral bandwidth to pass an up-converting frequency multiplier chain.

June-Koo Rhee [7] , developed a differential phase shift keying (DPSK) in the optical frequency domain, a differential phase modulation is implemented between adjacent spectral elements for a femtosecond optical pulse using a spatial acousto optic modulator. Frequency

domain differential phase shift keying (FD-DPSK) modulation scheme is considered to achieve high data rate using terahertz band.

Ajito and Muramoto, discussed about 24 Gbit/s wireless data transmission at 300 GHz using a uni-travelling carrier photodiode (UTC-PD) emitter and Schottky barrier diode detector[8]. The design is fabricated for larger bandwidth. Amplitude shift keying (ASK) signal is transmitted using two laser diodes at 300 GHz and received without error.

## **2.2 REVIEW ON CHANNEL MODEL**

In [9], the authors have discussed about the wireless communication over indoor Terahertz (THz) channels. In the 0.1 – 10 THz band are a very high molecular absorption and spreading loss for the line-of-sight (LOS) links. For the non-line-of-sight (NLOS) propagation, a very high reflection loss depending on the shape, material, and roughness of the reflecting surface affects the THz wave propagation. By considering these peculiarities the LOS path, NLOS path and equivalent channel model is implemented based on Kirchhoff scattering theory and ray tracing algorithm. It proposed the capacity of channel model, which observe that the LOS component dominates the performance and for NLOS component it achieves 100 Gbps.

Piesiewicz, and Kleine-Ostmann [10], described the reflective properties of building materials found in a typical office environment. The angular dependent reflection coefficients of different building materials were determined using terahertz time domain spectroscopy in transmission geometry and Fresnel's equations, which is more efficient than a set of measurements in reflection geometry for different angles. Determines the refractive index and absorption coefficient for glass, plaster and wood materials.

In [11], the authors measured the frequency dependent refractive index and absorption coefficient of a variety of common building and plastic materials between 100 and 1000 GHz. Determines the roughness factor, refractive index and the absorption coefficient for woods, bricks, plastic and glass samples. The measurements are performed with conventional free-space THz spectrometer and fibers to direct the optical femtosecond pulses.

S. Priebe, M. Jacob and C. Jansen, presented the non-specular scattering at rough surfaces in the THz frequency range by means of the Kirchhoff scattering theory [12]. It illustrates the angular dependent scattering behavior of a rough surface for the three dimensional radiation and calculated the scattered power for single scattering point. It also calculated the total scattered power for multipath reflection by the implementation of Kirchhoff scattering in the ray tracing algorithm.

R. Piesiewicz and C. Jansen [13], described the reflectivity of smooth, optically thick materials and modeled with Fresnel equations. In case of materials with a rough surface, diffuse scattering reduces the power reflected in the specular direction. The modified Fresnel equations that model scattering in the specular direction. Determines the surface roughness for the plaster S1, plasterS2 and wall paper samples.

C. Jansen, S. Priebe, C. Moller and M. Jacob [14], investigated the influence of diffuse scattering at such high frequencies on the characteristics of the communication channel and its implications on the non-line-of-sight propagation path. The Kirchhoff approach is verified by an experimental study of diffuse scattering from randomly rough surfaces commonly encountered indoor environments using a fiber-coupled terahertz time-domain spectroscopy system to perform angle- and frequency-dependent measurements. It proposed the Kirchhoff approach into a self-developed ray tracing algorithm to model the signal coverage of a typical office scenario.

The molecular absorption can be calculated using HITRAN database developed by Harvard university. Rothman, Gordon, Brown and Brown updated the status of the 2012 edition of the HITRAN molecular spectroscopic compilation [15]. The HITRAN molecular absorption compilation is comprised of six major components structured into folders that are freely accessible on the internet. These folders consist of the traditional line-by-line spectroscopic parameters required for high-resolution radiative-transfer codes, infrared absorption cross-sections for molecules. This HITRAN simulation it determines the Absorption coefficient, Absorption Spectrum, Transmittance spectrum, Radiance spectrum for various molecules at any temperature.

# CHAPTER 3

## CHANNEL MODELING

The physical mechanisms governing a wireless transmission in the THz band are different from those which affect schemes operating in the lower frequency bands. Therefore, already existing channel models cannot be used for THz communications. So new method of channel modeling and capacity analysis for the terahertz communication is discussed in this chapter.

### 3.1 CHANNEL MODEL

Wireless channel model over the indoor terahertz channel is developed considering the molecular absorption and based on Kirchhoff scattering theory and ray tracing algorithm for LOS and NLOS propagation paths respectively.

#### 3.1.1 LINE OF SIGHT PROPAGATION

The propagation model for communications in the THz band for LOS conditions has been developed. This model accounts for the total path loss that an EM wave in the THz band suffers from due to absorption and spreading loss when propagating over very short distances.

Spreading loss is the loss in signal strength of an electromagnetic wave, which attenuates the transmitted signal over distance because the signal is being spread over a larger and larger area. This attenuation is called spreading loss. Spreading loss is directly proportional to the frequency of the signal and the distance between the transmitter and receiver.

The (free space) spreading  $A_{spread}(f, r)$  loss accounts for the loss due to the expansion of the wave as it propagates through the medium at a distance  $r$  is given by,

$$A_{spread}(f, r) = \frac{(4\pi fr)^2}{c^2} \quad (1)$$

Absorption loss depends on the signal frequency and the atmospheric gases. In the THz band, the absorption level of atmospheric gases is very strong which is caused by molecular resonances

primarily due to water vapor and oxygen. The molecules in the air absorb the signal energy as it propagates through the air [3]. This attenuation is called atmospheric attenuation. Absorption coefficient  $\alpha_{molec}(f, T_K, p)$  is the necessary parameter for calculating absorption loss. Calculated the absorption coefficient using the HITRAN (High resolutions and transmission) simulation which influences the parameter temperature, frequency and pressure of the air.

The total attenuation that an EM wave of a frequency  $f$  suffers from due to molecular absorption when traveling over a distance  $r$  is given by,

$$A_{abs}(f, r) = e^{\alpha_{molec}(f, T_K, p)r} \quad (2)$$

The total path loss  $A^{dB}(f, r)$  can be expressed as the sum of the molecular absorption loss and spreading loss in

$$\begin{aligned} A^{dB}(f, r) &= A^{dB}_{abs}(f, r) + A^{dB}_{spread}(f, r) \\ &= \alpha_{molec}(f, T_K, p)r 10 \log_{10} e + 20 \log_{10} \left( \frac{4\pi fr}{c} \right) \end{aligned} \quad (3)$$

### 3.1.1.1 HITRAN

HITRAN is an acronym for High Resolution Transmission is a compilation of spectroscopic parameters that a variety of computer codes use to predict and simulate the transmission and emission of light in gaseous media including the atmosphere, laboratory cells, etc. The original version was compiled by the Air Force Cambridge Research Laboratories (1960s). HITRAN is maintained and developed at the Harvard-Smithsonian Center for Astrophysics, Cambridge MA, USA.

HITRAN is the worldwide standard for calculating or simulating atmospheric molecular transmission and radiance from the microwave through ultraviolet region of the spectrum. The current version contains 47 molecular species along with their most significant isotopologues. These data are archived as a multitude of high-resolution line transitions, each containing many spectral parameters required for high-resolution simulations [10]. In addition there are about 50 molecular species collected as cross-section data. These latter include anthropogenic constituents in the atmosphere such as the chlorofluorocarbons.

The spectrum of molecular gases is computed by the line-by-line models of spectral calculation in HITRAN compilation.

Molecules absorb and emit radiation only at certain discrete frequencies or wave numbers, corresponding to allowable changes in their quantum energy levels. This produces a unique spectrum for each gas species. It consists of several quantities they are wave number ( $cm^{-1}$ )  $\nu$ , transmittance  $\tau_\nu$ , emissivity  $\varepsilon_\nu$ , absorptivity  $\alpha_\nu$ .

Kirchhoff's law equates the absorptivity to emissivity at each wave number. Further, in the absence of scattering or reflections, the absorptivity is the complement of the transmittance. Each line in the absorption spectrum has a certain width and depth, and is centered at a particular wave number. The line positions and shapes are determined by the quantum mechanical properties of the molecule, and are affected by macroscopic conditions like pressure and temperature. The line parameters are derived by fitting a variety of laboratory spectra, measured over a range of conditions. Each absorption line is thereby characterized by a small set of parameters. With these parameters, an absorption line can be modeled at any given pressure, temperature and gas concentration. The collection of line parameters for a group of absorption lines is called a line list. For the simulation of the transmittance spectrum of a gas mixture in a given spectral range, the absorption lines of each gas must be calculated. Lines whose centers fall outside the spectral range, but whose wings extend into the range, must be included. The complete spectrum is effectively the product of the individual absorption line spectra. Algorithms that simulate molecular spectra in this way by accumulating the spectra of each individual absorption line are known as line-by-line models.

### 3.1.2 NON LINE OF SIGHT PROPAGATION

In an indoor scenario, the LOS propagation might be blocked by the presence of obstacles like moving people, furniture, or many diverse objects. For this case, the NLOS propagation will play an important role for enabling a stable wireless transmission and it is developed based on the Kirchhoff scattering theory and ray tracing model.

The reflection loss is depends on the properties of indoor building materials[10], such as roughness of the surface  $\sigma_{hs}$ , and correlation length  $l_{corr}$ . The scattering of the EM waves at rough surfaces in the THz band is modeled by means of Kirchhoff scattering theory.

### 3.1.2.1 KIRCHHOFF SCATTERING THEORY

Kirchhoff scattering theory starting from the Helmholtz integral, Beckmann and Spizzichino derive an analytical description of the electromagnetic field scattered from a rough surface [13]. The characteristics of the reflection are derived by the scattering coefficient.

$$\rho = \frac{E_{sc}}{E_{ref}} \quad (4)$$

Where  $E_{sc}$  is the scattered electric field and  $E_{ref}$  is the electric field reflected in the direction of the specular reflection by a smooth, perfectly conducting surface.

The general scattering geometry is shown in Figure 3.1. A wave, which is incident on the rough surface under an angle  $\theta_1$ , is scattered into the direction given by the angles  $\theta_2$  and  $\theta_3$ .

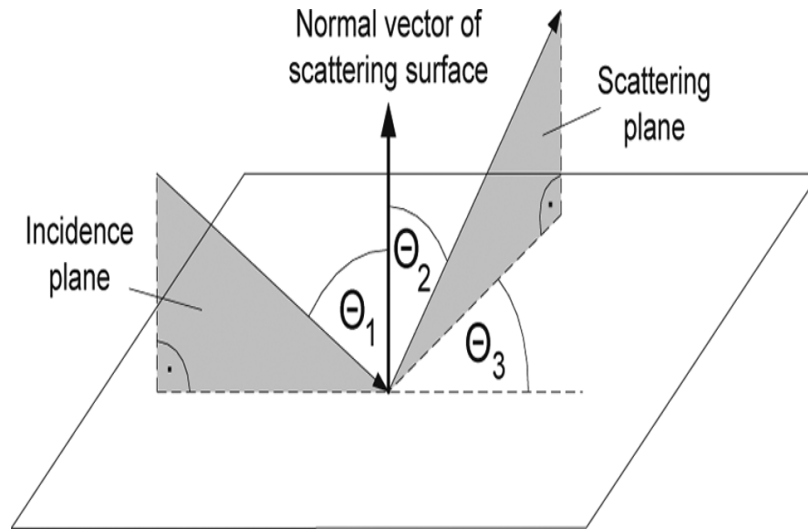


Figure 3.1. The basic geometry of scattering at a rough surface.

Specular means that the incident angle  $\theta_1$ , i.e., the angle between the incident ray and the surface normal, equals the reflected angle  $\theta_2$ , i.e., the angle between the reflected ray and the normal of the surface, and the angle  $\theta_3$ , defined for scattering directions that lie outside the plane of incidence equals to zero.

For an infinitely conductive surface of area A with dimension X and Y, the average scattering coefficient of an incident wave on a rough surface under an incident angle and scattered angles is computed by,

$$E\{\rho\rho^*\}_\infty = e^{-g} \left( \rho_0^2 + \frac{\pi l_{corr}^2 F^2}{A} \sum_{m=1}^{\infty} \frac{g^m}{m!m} e^{-v_{xy}^2 l_{corr}^2 / 4m} \right) \quad (5)$$

$$\text{With, } g = \sigma h s^2 (2\pi f / c)^2 (\cos\theta_1 + \cos\theta_2)^2,$$

$$\rho_0 = \sin c(v_x X) \cdot \sin c(v_y Y),$$

$$v_x = (2\pi f / c)(\sin\theta_1 - \sin\theta_2 \cos\theta_3),$$

$$v_y = (2\pi f / c)(-\sin\theta_2 \sin\theta_3),$$

$$v_{xy} = \sqrt{v_x^2 + v_y^2},$$

$$F = \frac{1 + \cos\theta_1 \cos\theta_2 - \sin\theta_1 \sin\theta_2 \cos\theta_3}{\cos\theta_1 (\cos\theta_1 + \cos\theta_2)}.$$

The mean scattering coefficient is the sum of two terms. The first term  $e^{-g}\rho_0^2$  is the specular spike component of the specular reflection, whereas the second term corresponds to the specular lobe, i.e., the diffusely scattered field that results from the roughness of the surface and is distributed around the specular spike. For small values of g the specular spike is very strong. As the roughness measure g increases, the magnitude of the lobe component increases relative to the spike component.

The mean scattering coefficient for finite conductors is obtained by average the Fresnel reflection coefficient  $\gamma$  over the entire surface area and utilize the resulting value  $E\{\gamma\gamma^*\}$  as a constant in the Helmholtz integral. Therefore, the scattering coefficient for finite conducting surfaces is obtained as,

$$E\{\rho\rho^*\}_{finite} = E\{\gamma\gamma^*\} E\{\rho\rho^*\}_\infty \quad (6)$$

The average power reflection coefficient of a surface area A, describing the scattered power in a distance  $r_0$  with respect to the incident power is given by,

$$E\{R_{power}\} = \left( \frac{fA \cos\theta_1}{cr_0} \right)^2 E\{\rho\rho^*\}_{finite} \quad (7)$$



### 3.1.2.2 RAY TRACING ALGORITHM

The non-specular scattering from rough surfaces will influence the broadband channel behavior. This effect is modeled by the implementation of the Kirchhoff model in a ray tracing algorithm [12]. Ray tracing algorithm is developed for calculating total scattered power for multipath propagation.

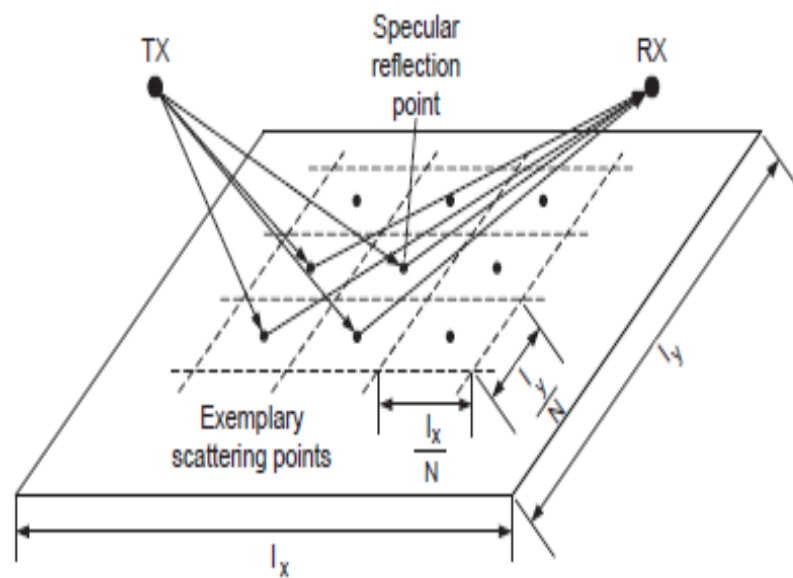


Figure 3.2 Division of the scattering surface in square tiles

#### Steps of ray tracing algorithm

- The entire surface area  $A = l_x.l_y$ , is separated into smaller square tiles as Figure 3.2.
- Determination of the specular reflection points.
- Placement of scattering tiles around each specular reflection point
- Computation of the geometrical parameters like incidence and emergent angles for each surface tile.
- Calculation of the individual powers of the rays scattered from the tiles according to the Kirchhoff equations.
- Summed up in order to obtain the total scattered power.

### 3.1.3 EQUIVALENT CHANNEL MODEL

The equivalent deterministic channel model has been developed for an indoor environment, which captures the direct ray as well as indirect (or reflected) rays from rough surface scattering.

The equivalent channel transfer function is given by,

$$H^{EQ}(f, r, \zeta) = H^{LOS}(f, r)e^{-j2\pi f\tau_{LOS}} + \sum_{i=1}^{M_{rays}} H_i^{NLOS}(f, \zeta_i)e^{-j2\pi f\tau_{NLOS_i}} \quad (8)$$

Where  $M_{rays}$  is the number of indirect rays,  $\tau_{LOS} = r/c$  and  $\tau_{NLOS_i} = \frac{r_{i1} + r_{i2}}{c}$  are the propagation delays of the LOS path and  $i^{th}$  NLOS path, respectively, with  $r$  denoting the distance between the TX and RX,  $r_{i1}$  the distance between the TX and the  $i^{th}$  scattering point and  $r_{i2}$  is the distance between the  $i^{th}$  scattering point and the RX. The vector  $\zeta = [\zeta_1, \dots, \zeta_{M_{rays}}]$  describes the coordinates of all the scattering points, where  $\zeta_i = [r_{i1}, r_{i2}, \theta_{i1}, \theta_{i2}, \theta_{i3}]$  defines the parameters of the  $i^{th}$  scattering point location.

The magnitude of the LOS path,

$$H^{LOS}(f, r) = H_{spread}(f, r) \cdot H_{abs}(f, r) \quad (9)$$

With

$$H_{spread}(f, r) = \frac{c}{4\pi fr}$$

$$H_{abs}(f, r) = e^{-\frac{1}{2}\alpha_{molec}(f, T_K, P)r}$$

The  $i^{th}$  NLOS path coefficient is defined as,

$$H_i^{NLOS}(f, r, \zeta_i) = H_{ref,i}(f, r_{i2}, \theta_{i1}, \theta_{i2}, \theta_{i3}) \times H_{spread,i}(f, r_{i1}, r_{i2}) \cdot H_{abs,i}(f, r_{i1}, r_{i2}) \quad (10)$$

With

$$H_{ref,i}(f, r_{i2}, \theta_{i1}, \theta_{i2}, \theta_{i3}) = \sqrt{E\{R_{power,i}(f, r_{i2}, \theta_{i1}, \theta_{i2}, \theta_{i3})\}}$$

$$H_{spread,i}(f, r_{i1}, r_{i2}) = \frac{c}{4\pi f (r_{i1} + r_{i2})}$$

$$H_{abs,i}(f, r_{i1}, r_{i2}) = e^{-\frac{1}{2}\alpha_{molec}(f, T_K, p)(r_{i1} + r_{i2})}$$

The equivalent channel transfer function (CTF) highly depends on the geometry of the specific propagation environment, i.e., the position of the TX and RX.

### 3.2 Capacity Analysis

The channel transfer function  $H^{EQ}(f, r, \zeta)$  is highly frequency selective. So, the total bandwidth  $B$  is divided into  $N$  narrow sub-bands of equal width  $\Delta f = \frac{B}{N}$ . Each sub channel is modeled as a frequency non selective. The total capacity is the sum of individual capacity of each sub bands.

The total channel capacity is given by,

$$C(f, r, \zeta) = \Delta f \sum_{i=1}^N \log_2 \left( 1 + \frac{\Phi_T(f_i, r, \zeta) |H^{EQ}(f_i, r, \zeta)|^2}{\Phi_N(f_i, r)} \right) \quad (11)$$

Where  $\Phi_T(f, r, \zeta)$  is the power spectral density (PSD) of the transmitted signal and  $\Phi_N(f, r)$  is the noise power spectral density.

There are two main noise sources in the terahertz band they are molecular absorption noise and the thermal noise. The noise power spectral density (PSD) of the molecular absorption noise is given by,

$$\Phi_{mol}(f, r) = k_B T_{mol}(f, r) \quad (12)$$

Where  $k_B = 1.3806 \times 10^{-23} \text{ J / K}$  the Boltzmann constant and the molecular noise temperature are is  $T_{mol}(f, r) = T_0(1 - e^{-\alpha_{mol}(f, TK, p)r})$  with  $T_0 = 296\text{k}$  reference temperature. The noise PSD of the thermal noise is given for high frequency as,

$$\Phi_{thermal}(f) = \frac{hf}{\exp\left(\frac{hf}{k_B T_0}\right) - 1} \quad (13)$$

Where  $h = 6.6262 \times 10^{-34} \text{ Js}$  is the Planck's constant.

The total noise power spectral density is obtained as,

$$\Phi_N(f, r) = \Phi_{mol}(f, r) + \Phi_{thermal}(f, r) \quad (14)$$

The power spectral density of the transmitted signal for each sub band is calculated using water filling algorithm such that it satisfies the condition,

$$\Phi_T(f_i, r, \zeta) = \left( \mu - \frac{\phi_N(f_i, r)}{|H^{EQ}(f_i, r, \zeta)|^2} \right) \quad (15)$$

Where  $\mu$  the water level is is computed using the condition,

$$\Delta f \left( \sum_{i=1}^N \left( \mu - \frac{\Phi_N(f_i, r)}{|H^{EQ}(f_i, r, \zeta)|^2} \right) \right) = P \quad (16)$$

With the total transmit power  $P$ . A typical transmit power for the terahertz band is between 1mW and 1W.

Wireless channel transfer function in the THz frequency consists of two components. The first one LOS path modeled using HITRAN simulation tool which primarily accounts for molecular absorption and spreading loss. Second one NLOS path modeled using Kirchhoff scattering theory and ray tracing algorithm. Further, equivalent channel is developed by considering these both LOS and NLOS path. The capacity of channel is analyzed by the summation of individual capacity of each sub bands.

# **CHAPTER 4**

## **MODULATION SCHEMES**

In this chapter the modulation schemes for the performance analysis of the ultrafast terahertz communication have been discussed.

### **4.1 MODULATION**

Modulation plays a key role in communication system to encode information digitally in analog world. It is very important to modulate the signals before sending them to the receiver section for larger distance transfer, accurate data transfer and low-noise data reception.

Modulation is a process of changing the characteristics of the wave to be transmitted by superimposing the message signal on the high frequency signal. In this process video, voice and other data signals modify high frequency signals – also known as carrier wave. This carrier wave can be DC or AC or pulse chain depending on the application used. Usually high frequency sine wave is used as a carrier wave signal.

These modulation techniques are classified into two major types they are analog and digital or pulse modulation.

In analog modulation, a continuously varying sine wave is used as a carrier wave that modulates the message signal or data signal. The Sinusoidal wave's is used as a general function in which, three parameters can be altered to get modulation – they are amplitude, frequency and phase.

In digital modulation, a message signal is converted from analog to digital message, and then modulated by using a carrier wave. For a better quality and efficient communication, digital modulation technique is employed. The main advantages of the digital modulation over analog modulation include permissible power, available bandwidth and high noise immunity. Digital modulation technique is classified into three types they are Amplitude Shift Keying (ASK), Frequency Shift Keying (FSK), and Phase Shift Keying (PSK).

## **DQPSK**

Phase-shift keying (PSK) is a digital modulation scheme that conveys data by changing the phase of a reference signal. Differential Phase Shift Keying (DPSK) is the version of binary phase shift keying (BPSK). In DPSK, there is no absolute carrier phase reference, instead transmitted signal itself used as phase reference. In differentially encoded QPSK (DQPSK), the phase-shifts are  $0^\circ$ ,  $90^\circ$ ,  $180^\circ$ ,  $-90^\circ$  corresponding to data '00', '01', '11', '10'. This kind of encoding may be demodulated in the same way as for non-differential PSK but the phase ambiguities can be ignored. Thus, each received symbol is demodulated to one of the M points in the constellation and a comparator then computes the difference in phase between this received signal and the preceding one.

### **4.1.1 PULSE MODULATION SCHEME**

The terahertz communication is performed by modulate the spectral domain of the femtosecond pulse with the phase of the input symbols called as frequency domain differential phase shift keying (FD-DPSK) .

Femtosecond pulse is a ultrashort rectangular pulse whose time duration is of the order of a picoseconds  $10^{-12}$  or less. Such pulses have a broadband spectrum, so femtosecond pulse is preferable for the ultrafast terahertz communication.

#### **4.1.1.1 FD-DQPSK MODULATION**

The frequency domain differential quadrature phase shift keying (FD-DQPSK) is developed based on FD-DPSK.

In the modulation process, n input symbols are considered  $a_1, a_2, a_3, \dots, a_n$ , where the input symbol  $a_i \in \{1, 2, 3, 4\}$ . The input symbols 1, 2, 3, 4 are corresponds to bit sequences as 00, 01, 11, 10 respectively. Since DPSK modulation is used, the transmitter needs to send an extra symbol as a reference phase. Therefore, the spectrum of the femtosecond pulse signal is sliced into  $n + 1$  band.

The phase function for each of these symbols is,

$$\psi(a_i) = \begin{cases} 0 & \text{for } a_i = 1 \\ \frac{\pi}{3} & \text{for } a_i = 2 \\ \frac{2\pi}{3} & \text{for } a_i = 3 \\ \pi & \text{for } a_i = 4 \end{cases} \quad (1)$$

Then the corresponding  $n + 1$  phases are obtained as,

$$\phi_i = \begin{cases} 0 \\ \psi(a_i) + \phi_{i-1} \end{cases} \quad \text{for } i=1,2,3..n \quad (2)$$

Where  $\phi_0$  is the reference phase.

The transmitter block diagram of the FD-DPSK is shown in the Figure 4.1. In the transmitter part the femtosecond ultrashort pulse is generated as a step rectangular pulse which corresponds to a sinc function in the frequency domain with 1.2 THz bandwidth. The spectrum of the pulse is sliced into  $n + 1$  bands and each band is modulated with phase of the  $n + 1$  transmitted symbols.

Each band is modulated as,

$$E(f) = \sum_{i=0}^n \exp(j\phi_i) S(f - f_i, \delta f) \quad (3)$$

Where  $E(f)$  the spectral complex value of the femtosecond signal is,  $i$  corresponds to the each spectral band and  $S(f - f_i, \delta f)$  is the spectral value of the  $i$  th band. Here, it noted that,  $f_i = f_0 + \delta f$  is the central frequency of the each band,  $\delta f = \Delta f / n + 1$  is the bandwidth of each  $i$  th band and  $f_0$  is the central frequency of the first spectral band of the femtosecond signal spectrum of bandwidth  $\Delta f$ .

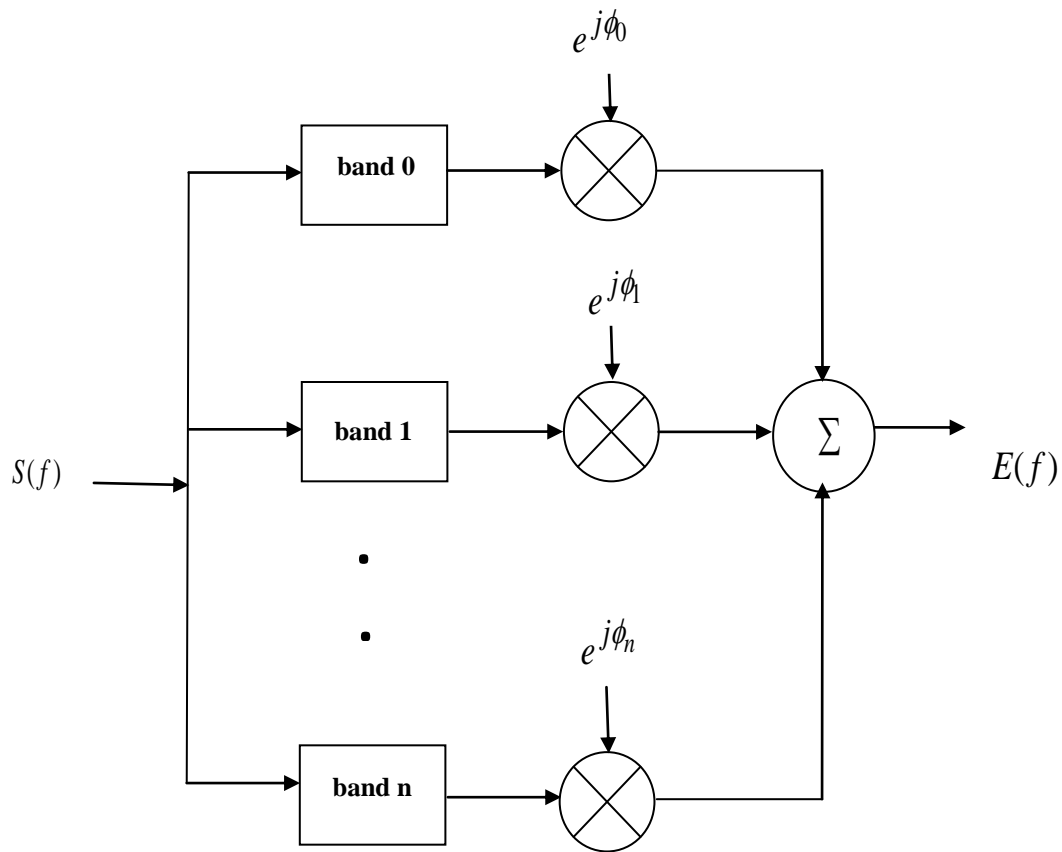


Figure 4.1 Transmitter block diagram

The modulated signal  $E(f)$  is then passed through the terahertz channel and is changed based on the channel characteristics. The input signal  $E(f)$  is multiplied by the channel transfer function  $H(f)$  and the noise is added to the result. For noise, standard model of Gaussian noise is used.

Therefore the received signal is obtained as,

$$R(f) = E(f)H(f) + noise \quad (4)$$



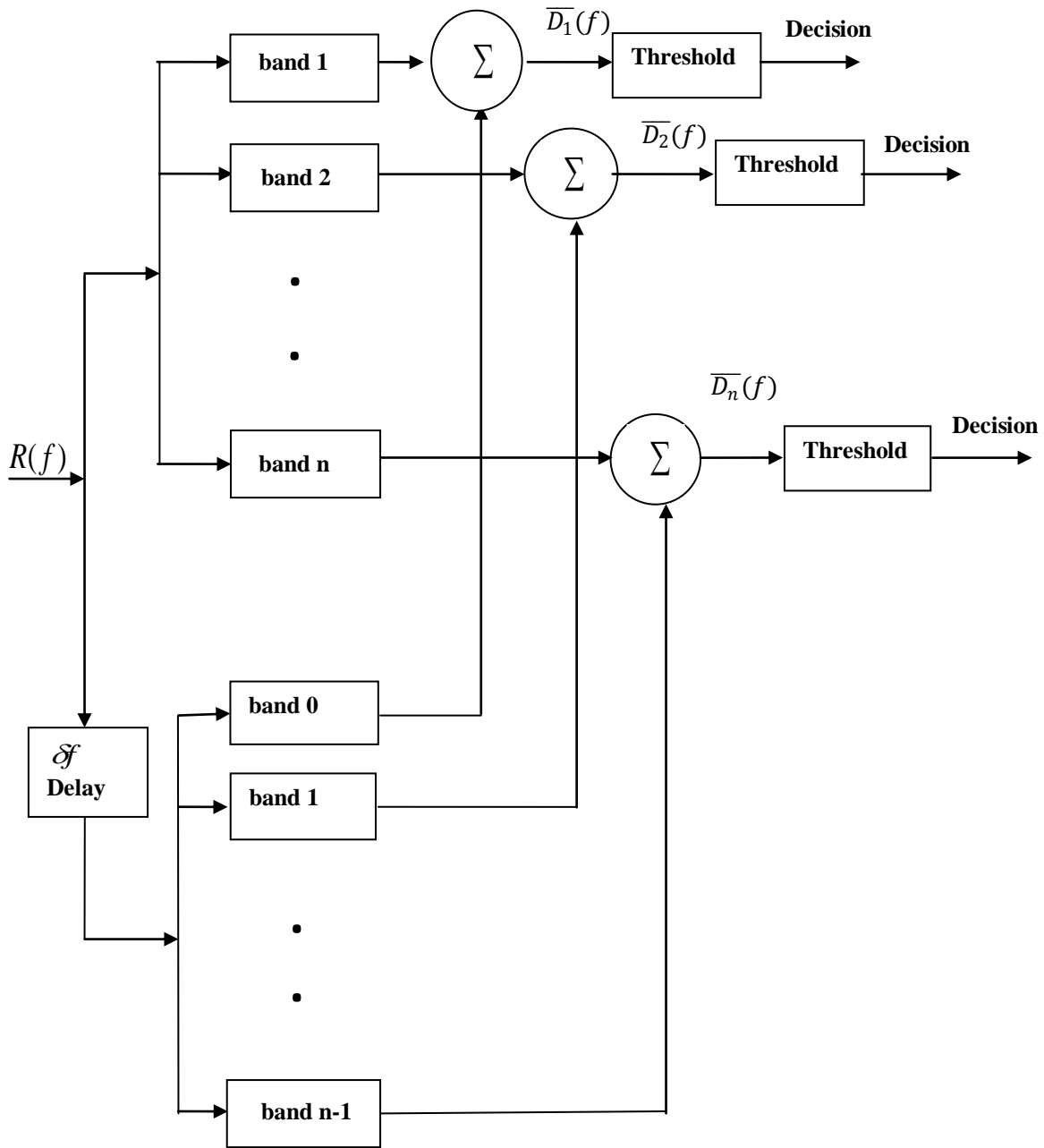


Figure 4.2 Receiver block diagram

The receiver block diagram is shown in the Figure 4.2. The received signal  $R(f)$  is sliced into  $n + 1$  band. A copy of the signal is shifted in frequency by  $\delta f$ . Thus the shifted  $(i - 1)$  th band has the central frequency of the unshifted  $i$  th band. Then the  $i$  th band of the unshifted signal is combined with the  $(i - 1)$  th band of shifted signal obtained as,

$$\overline{D}_i(f) = \frac{1}{2} [R'(f - f_{i-1}, \delta f) + R(f - f_i, \delta f)] \quad (5)$$

$$\text{for } i = 1, 2, 3, \dots, n$$

Where  $R(f - f_i, \delta f)$  is the  $i$  th band of the received signal, and  $R'(f - f_i, \delta f)$  is the  $i$  th band of the received signal that is shifted by  $\delta f$ .

The intensity of the  $\overline{D}_i(f), |\overline{D}_i(f)|^2$  are compared with the different threshold values at the receiver. The threshold values are found based on the following equations,

$$\overline{E}_i(f) = \frac{1}{2} [\exp(j\phi_{i-1})S(f - f_{i-1}, \delta f) + \exp(j\phi_i)S(f - f_i, \delta f)] \quad (6)$$

$$\text{for } i = 1, 2, 3, \dots, n$$

$$|\overline{E}_i(f)|_{a_i}^2 = \frac{1}{2} |\overline{S}_i(f)|^2 \times |1 + \exp(2j\psi(a_i)) + 2\exp(j\psi(a_i))| \quad (7)$$

$$\text{for } i = 1, 2, 3, \dots, n$$

Here,  $\overline{S}_i(f)$  is the average of each two consecutive unmodulated spectral bands and is obtained as,

$$\overline{S}_i(f) = \frac{1}{2} [S(f - f_{i-1}, \delta f) + S(f - f_i, \delta f)] \quad (8)$$

$$\text{for } i = 1, 2, 3, \dots, n$$

Since we using DQPSK,  $|\overline{E}_i(f)|^2$  can be simplified for each  $a_i$  symbols as,

$$|\overline{E}_i(f)|^2 = \begin{cases} |\overline{S}_i(f)|^2 & \text{for } a_i = 1 \\ \frac{3}{4}|\overline{S}_i(f)|^2 & \text{for } a_i = 2 \\ \frac{1}{4}|\overline{S}_i(f)|^2 & \text{for } a_i = 3 \\ 0 & \text{for } a_i = 4 \end{cases} \quad (9)$$

The threshold values for each symbol is given by,

$$th1_i = \frac{|\overline{S}_i(f)|^2 + \frac{3}{4}|\overline{S}_i(f)|^2}{2} = \frac{7}{8}|\overline{S}_i(f)|^2 \quad (10)$$

$$th2_i = \frac{\frac{3}{4}|\overline{S}_i(f)|^2 + \frac{1}{4}|\overline{S}_i(f)|^2}{2} = \frac{4}{8}|\overline{S}_i(f)|^2 \quad (11)$$

$$th3_i = \frac{\frac{1}{4}|\overline{S}_i(f)|^2 + 0}{2} = \frac{1}{8}|\overline{S}_i(f)|^2 \quad (12)$$

The received symbols  $r_i$  are detected by comparing these thresholds values with the intensity values of  $|\overline{D}_i(f)|^2$  as,

$$r_i = \begin{cases} 1 & \text{if } |\overline{D}_i(f)|^2 \geq th1_i \\ 2 & \text{else if } |\overline{D}_i(f)|^2 \geq th2_i \\ 3 & \text{else if } |\overline{D}_i(f)|^2 \geq th3_i \\ 4 & \text{otherwise} \end{cases} \quad (13)$$

#### 4.1.1.1 ADAPTIVE FD-DQPSK MODULATION

In the FD-DPSK modulations for terahertz communication, some bands are attenuated due to humidity in the air this causes the high symbol error rate (SER). Therefore, by excluding these erroneous bands from the modulation, lower SER is achieved for the same energy per bit to the spectral noise density. This technique is called adaptive FD-DPSK modulation scheme. In adaptive method, the number of symbols that are sent in each femtosecond pulse is decreased proportionally to the number of deleted bands.

##### Steps for Adaptive modulation

1. The available bands in the system are categorized into two groups; they are error free bands and erroneous bands.
  - i. Error free bands- Bands that will carry the useful information and it cannot be attenuated.
  - ii. Erroneous bands- the band which are attenuated due to humidity and it should be excluded from the modulation.
2. At the transmitter,
  - i. The phase corresponding to error free bands are founds as FD-DPSK modulation scheme.
  - ii. The phases corresponding to erroneous bands are set to 0.
  - iii. The superposition of the phases of both error free and erroneous bands is used to modulate the pulses.
3. At the receiver side, the erroneous bands will be ignored and the remaining error free bands are used for detect the received symbols.

The set of bands that are excluded depends on the distance between the Tx and Rx as well as the humidity. Thus, at lower humidity or smaller distances, fewer bands are excluded, since the attenuation is not significant. At larger distances or higher humidity, more number of bands are excluded, therefore the corresponding transmitted symbols are deleted. Hence, the symbol error rate for larger distances is higher than the short distances.

## CHAPTER 5

### SIMULATION RESULTS

The simulation results including the channel characteristic, performance of the channel with pulsed modulation schemes are discussed in this chapter. The parameters considered for the simulation of channel model for terahertz communication are listed in the table below.

Table 5.1 Simulation parameters

<b>Parameters</b>	<b>Values</b>
Frequency	0.1-10 THz
Temperature(in Kelvin)	278K,308K
Pressure	1ppm

The absorption characteristics of terahertz channel are modeled using **HITRAN** simulation for 278 Kelvin and 308 Kelvin are shown in Figure 5.1 and 5.2 respectively. The absorption coefficient depends on temperature, frequency and pressure of the water vapors. The absorption characteristics are plotted with respect to the wave numbers. The wave number is indirectly proportional to frequency. The frequency range of these models is 0.1THz to 10 THz.

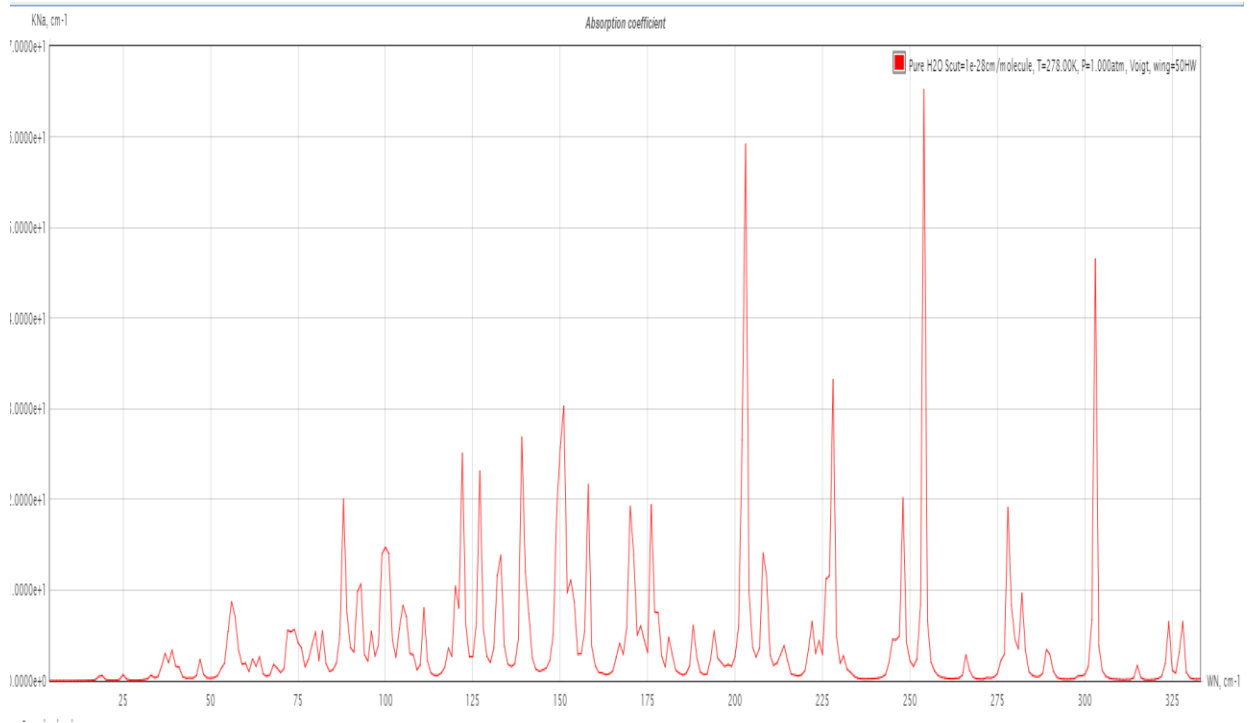


Figure 5.1 Absorption coefficient Vs Wave number for 278 Kelvin

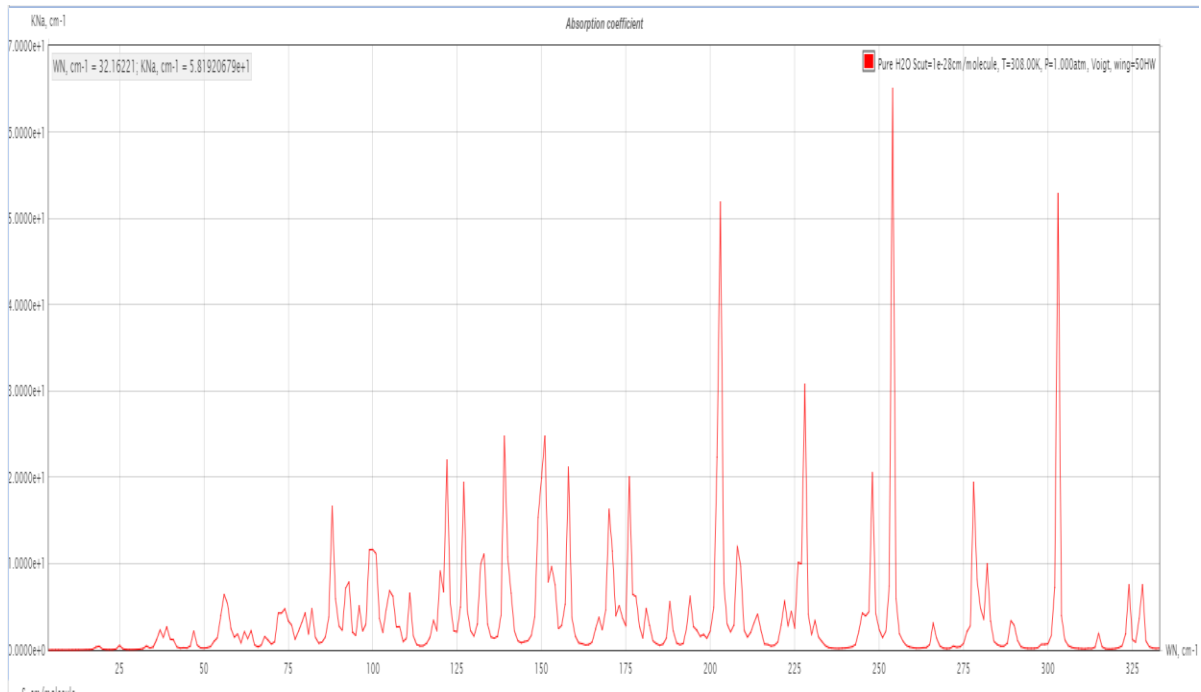


Figure 5.2 Absorption coefficient Vs Wave numbers for 308 Kelvin

The absorption coefficient is a strong function of wavelength. At some specific wavelengths the absorption coefficient is very high. Absorption coefficient slightly varies with temperature also. The absorption coefficient increases with decreases in temperature. But variation is very less compared to the variation of absorption coefficient with frequency. For both 278 Kelvin and 308 Kelvin, the absorption coefficient is maximum at the wavelength 255.

The total Line Of Sight path loss is modeled for 278 Kelvin and 308 Kelvin using equation (3) of chapter 3 over the frequency range of (0.1 – 10) THz is shown in Figure 5.3 and 5.4 respectively.

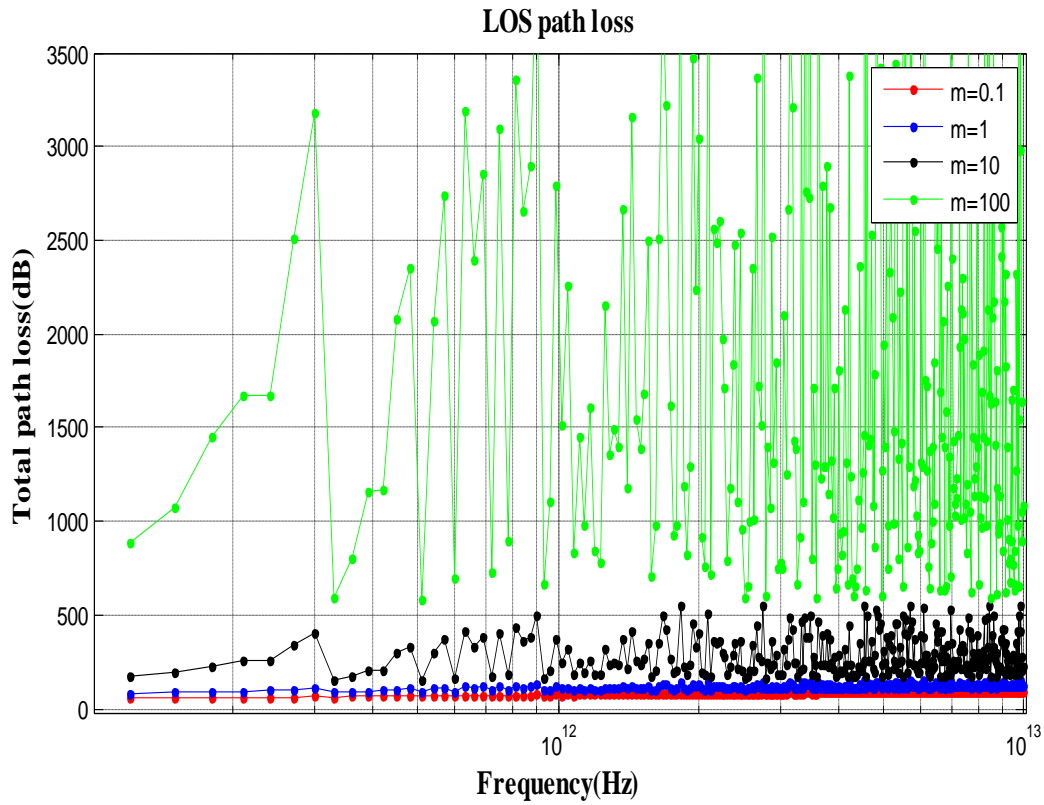


Figure 5.3 Total path losses Vs Frequency for 278 Kelvin



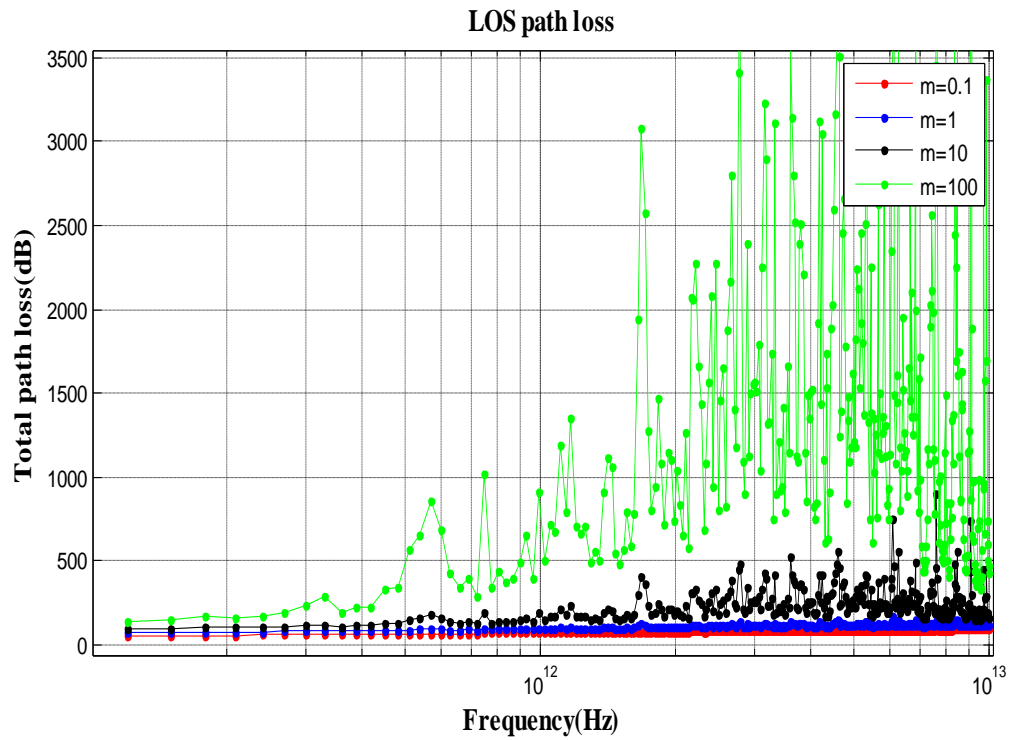


Figure 5.4 Total path losses Vs Frequency for 308 Kelvin

Path loss for distance of 0.1 m, 1m 10m and 100m are calculated and as expected the path loss is a very strong function of distance. From these results, it is also clear that the total path loss at 278 Kelvin is more than that of 308 Kelvin.

The reflection power characteristics for the terahertz channel is modeled using kirchoff scattering theory and ray tracing algorithm using equation (7) of chapter 3 for the frequency range of (0.1-1)THz as shown in the Figure 5.5



Figure 5.5 Reflection power Vs Frequency

The reflected power of the non line of sight propagation path (NLOS) is observed as 26dB to -100dB. It infers that for higher frequency value the reflection loss is maximum.

The equivalent channel model for the indoor office room have been modeled over the frequency range of (0.1-10) THz range using equation (8) of chapter 3 is shown in the Figure 5.6. This model accounts for both line of sight propagation path and non line of sight propagation path.

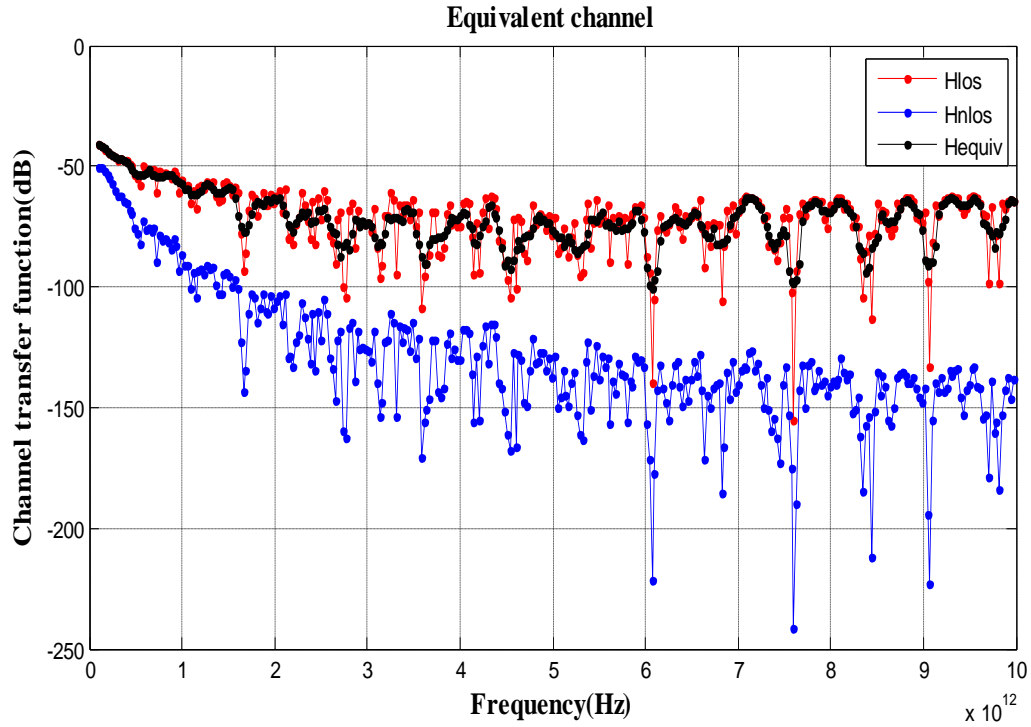


Figure 5.6 Channel Transfer Function Vs Frequency

Due to the constructive and destructive superposition of the numerous reflected paths and the direct path, fluctuations of the channel transfer functions are observed. The simulation result of this indoor scenario infers the LOS component dominates and exhibits a path gain of -41 dB to -70 dB.

The average capacity for LOS path, NLOS path, equivalent path of terahertz channel is simulated for the frequency range (0.1-1) THz over the distance range of 0.5 to 5 meters using equation (11) in chapter 3 as shown in the Figure 5.7.

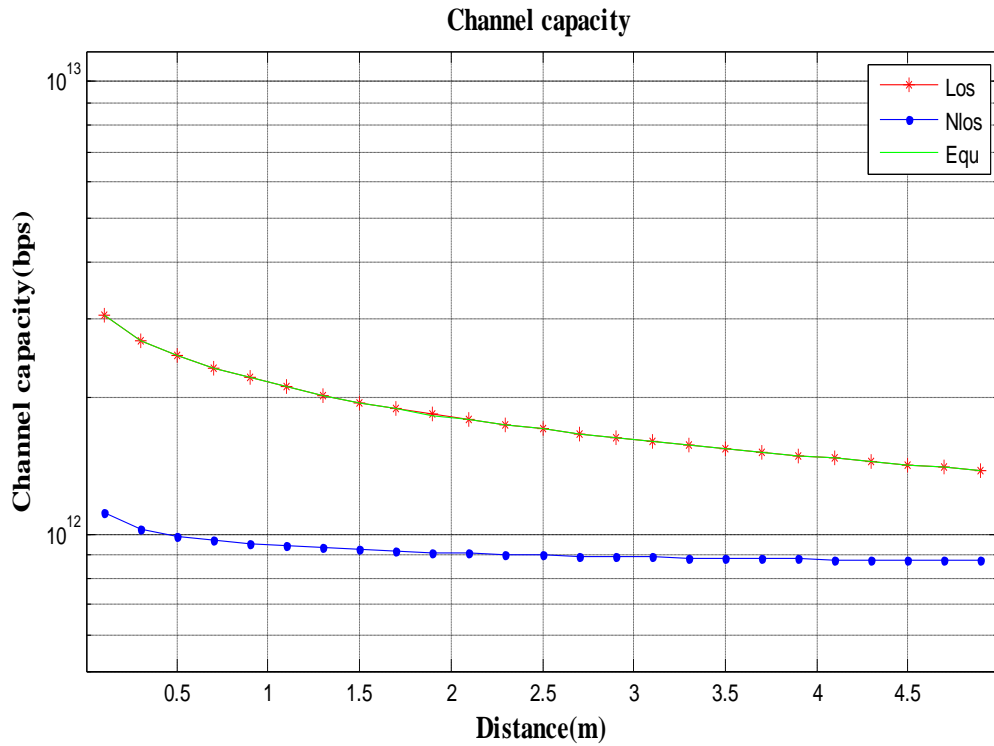


Figure 5.7 Average Channel Capacity for LOS, NLOS, Equivalent path

From these results, it observes that the LOS path achieves the data rate in the range of 3 Terabits per second (Tbps). For NLOS path it achieves around 1 Tbps.

The ultrafast pulsed terahertz communication is developed by FD-DQPSK modulation and adaptive FD-DQPSK modulation schemes. The symbol error rate (SER) performance of each of these modulation schemes for the distances of 0.5m and 10 cm is shown in the Figure 5.8.

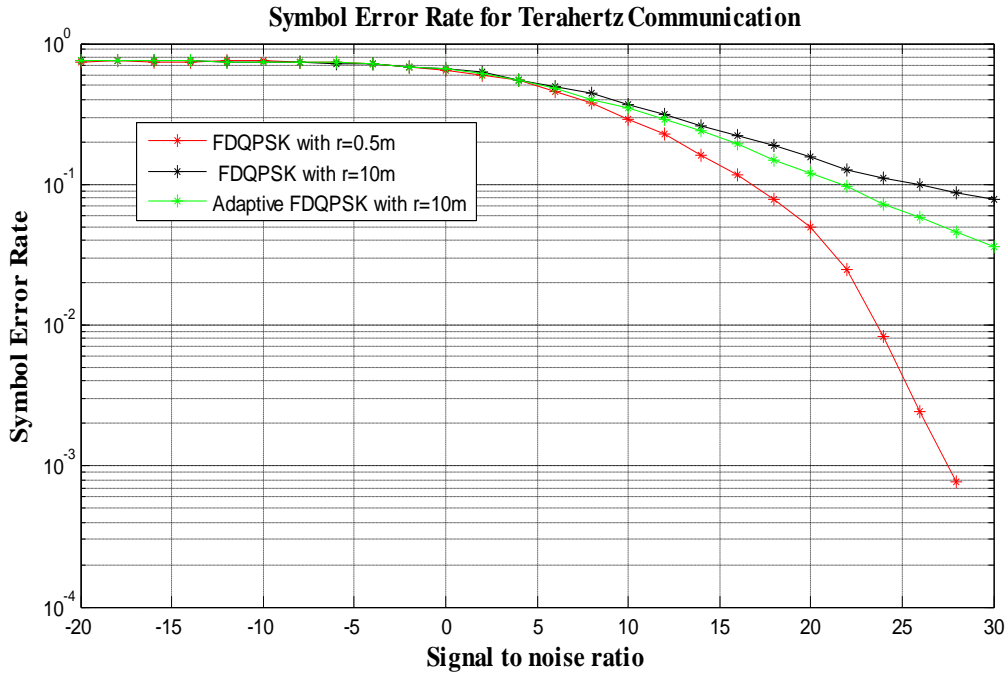


Figure 5.8 SER for FD-DQPSK and adaptive FD-DQPSK

From these results, it observes that adaptive modulation exhibits the lower SER than the FD-DQPSK modulation. And also, it clears that for the distance of 10 m the SER is higher than the 0.5 m distance. It infers that for larger distances the SER is increases.

# **CHAPTER 6**

## **CONCLUSION AND FUTURE WORK**

### **CONCLUSION**

Terahertz communication is used to satisfy the increasing demands for higher data rates. Wireless transmission in the 0.1 – 10 THz band obtains a very high molecular absorption and spreading loss. Due to these characteristics the channel in this THz band is considered different from lower frequency band. Therefore, already existing channel models cannot be re-used for THz communications. The absorption loss and the reflection loss for the LOS propagation path and NLOS propagation path are analyzed in this thesis. By considering these two paths equivalent channel model is developed based on Kirchhoff scattering theory and ray tracing algorithm. The performance of channel transfer function (CTF) of the channel model is accomplished. The simulation result shows that CTF of LOS path dominates and exhibits over the entire band from 0.1 THz to 10 THz a path gain of 41dB to -70dB. The capacity of this channel achieves the data rate in the range of Tbps. Furthermore, ultrafast pulsed terahertz communication is developed based on FD-DQPSK modulation. In terahertz channel, absorption loss due to water vapor leads to high symbol error rate (SER). The adaptive FD-DQPSK modulation method is implemented based on Tx-Rx distance and humidity of the channel, the system excludes some bands from the modulation scheme. By utilizing the adaptive method it enhances the symbol error rate (SER).

### **FUTURE WORK**

The pulsed terahertz communication is limited for the larger distances. The distance can be improved by implementing distance-aware bandwidth-adaptive resource allocation scheme in terahertz communication.

## REFERENCES

- [1] I.Akyildiz, J.Jornet, and C.Han, “Terahertz band: Next frontier for wireless communications”, *Physical Communication*, vol. 12, pp. 16–32, 2014.
- [2] H. Song and T. Nagatsuma, “Present and future of terahertz communications”, *IEEE Transactions on Terahertz Science and Technology*, vol. 1,no. 1, pp. 256–263, 2011.
- [3] Farnoosh Moshir, Suresh Singh,” Pulsed Terahertz Time-Domain Communication”, *Globecom wireless communication symposium*,2014.
- [4] Anamaria Moldovan, Steven Kisseleff, Ian F. Akyildiz, and Wolfgang H. Gerstacker, ” Data Rate Maximization for Terahertz Communication Systems using Finite Alphabets”, *IEEE ICC - Wireless Communications Symposium*,2016.
- [5] Cheng Wang, Changxing Lin, Qi Chen, Bin Lu, Xianjin Deng, and Jian Zhang, ” A 10-Gbit/s Wireless Communication Link Using 16-QAM Modulation in 140-GHz Band”, *IEEE Transactions on Microwave Theory and Techniques*, vol. 61, no. 7, July 2013.
- [6] Lothar Moeller, John Federici, Ke Su, “THz Wireless Communications: 2.5 Gb/s Error-free Transmission at 625 GHz using a Narrow-bandwidth 1 mW THz Source”, in *2011 XXXth URSI General Assembly and Scientific Symposium*, 2011, pp. 1–4.
- [7] June-Koo Rhee, Hisashi Kobayashi, and Warren S. Warren, “Optical frequency domain differential phase shift keying in femtosecond-pulse spectral modulation systems,” *Journal of Lightwave Technology*, vol. 15, no. 12, pp. 2214– 2222, 1997.
- [8] H.-J. Song, K. Ajito, Y. Muramoto, A. Wakatsuki,T. Nagatsuma and N. Kukutsu, “24 Gbit/s data transmission in 300 GHz band for future terahertz communications,” *Electronics Letters*, vol. 48, no. 15, pp. 953–954, July 2012.
- [9] Anamaria Moldovan, Michael A. Ruder, Ian F. Akyildiz, and Wolfgang H. Gerstacker, “LOS and NLOS Channel Modeling for Terahertz Wireless Communication with Scattered Rays”, *Proc. of the IEEE Globecom Emerging Technologies for 5G Wireless Cellular Networks Workshop*, pp. 388–392, 2014.
- [10] R. Piesiewicz, T. Kleine-Ostmann, N. Krumbholz, D. Mittleman, M.Koch, and T. Kürner, “Terahertz characterisation of building materials”, *Electronics Letters*, vol. 41, no. 18, pp. 1002–1004, 2005.

- [11] R. Piesiewicz, C. Jansen, S. Wietzke, D. Mittleman, M. Koch, and T. Kürner, “Properties of building and plastic materials in the THz range”, *International Journal of Infrared and Millimeter Waves*, vol. 28, no. 5, pp. 363–371, 2007.
- [12] S. Priebe, M. Jacob, C. Jansen, and T. Kürner, “Non-specular scattering modeling for THz propagation simulations”, in *Proceedings of the 5th European Conference on Antennas and Propagation (EUCAP)*, IEEE, 2011, pp. 1–5.
- [13] R. Piesiewicz, C. Jansen, D. Mittleman, T. Kleine-Ostmann, M. Koch, and T. Kürner, “Scattering analysis for the modeling of THz communication systems”, *IEEE Transactions on Antennas and Propagation*, vol. 55, no. 11, pp. 3002–3009, 2007.
- [14] C. Jansen, S. Priebe, C. Moller, M. Jacob, H. Dierke, M. Koch, and T. Kürner, “Diffuse scattering from rough surfaces in THz communication channels”, *IEEE Transactions on Terahertz Science and Technology*, vol. 1, no. 2, pp. 462–472, 2011.
- [15] L. Rothman, I. Gordon, Y. Babikov, A. Barbe, L. Brown, P. Bernath, M. Birk, V. Boudon, L. Brown, A. Campargue, J.-P. Champion, et al., “The HITRAN 2012 molecular spectroscopic database”, *Journal of Quantitative Spectroscopy and Radiative Transfer*, vol. 130, no. 2013, pp. 4–50, 2013.



# LIST OF PUBLICATIONS

## CONFERENCES

- Presented a paper titled “**Channel Modeling Of Terahertz Wireless Communication**” in **ICMR** sponsored **IEEE International Conference on Science, Technology, Engineering and Management (ICSTEM’17)** held at KIT- Kalaignarkarunanidhi Institute of Technology, Coimbatore on March 3<sup>rd</sup> and 4<sup>th</sup> 2017.

# KIT - Kalaignarkarunanidhi Institute of Technology



(Accredited with 'A' Grade by NAAC)  
(Approved by AICTE, New Delhi & Affiliated to Anna University, Chennai)  
KIT Global Institute for Advanced Studies & Research  
Coimbatore-641 402, Tamilnadu, India.



## Certificate of Appreciation

This is to certify that *Dr./Mr./Ms./Prof* ..... **J. VANMATHI** .....  
of **KUMARAGURU COLLEGE OF TECHNOLOGY** ..... has presented  
a paper titled **CHANNEL MODELING FOR TERRA HERTZ** .....  
**WIRELESS COMMUNICATION** ..... in  
ICMR sponsored *IEEE International Conference on Science, Technology,  
Engineering and Management (ICSTEM'17)* held on 3<sup>rd</sup> and 4<sup>th</sup>  
March, 2017 at KIT - Kalaignarkarunanidhi Institute of Technology, Coimbatore,  
Tamilnadu, India.

**Dr. R. Sukumar**  
Organizing Chair

**Dr. P. Anbalagan**  
Director

**Dr. N. Mohan Das Gandhi**  
Principal

*In Association with*

